Inorganic Chemistry

Article

pubs.acs.org/IC

Changing Hafnium Speciation in Aqueous Sulfate Solutions: A High-Energy X-ray Scattering Study

Ali Kalaji,[†] S. Skanthakumar,[†] Mercouri G. Kanatzidis,[‡] John F. Mitchell,[‡] and L. Soderholm*[,†]

[†]Chemical Sciences and Engineering Division, [‡]Materials Science Division, Argonne National Laboratory, Argonne, Illinois 60439, United States

Supporting Information

ABSTRACT: The relationship of solution speciation and the structures of corresponding precipitates is examined for an aqueous Hf^{4+} sulfate series. High-energy X-ray scattering (HEXS) and Raman spectroscopy data are used to probe atomic correlations in solutions. Hf^{4+} in acidic perchlorate solution shows no evidence of a mononuclear metal species but instead has a peak in the pair-distribution function (PDF), generated from the HEXS data, at 3.55 Å, indicating Hf^{4+}–Hf^{4+} solution correlations. The peak intensity is consistent with clusters that are, on average, larger than the tetramic unit $[M_4(OH)_8(H_2O)_{16}]^{8+}$ usually attributed to Zr^{4+} and Hf^{4+} solution speciation under these conditions. Addition of sulfate results in a breakup of hydroxo-bridged oligomers into sulfate-capped dimers and, for higher concentrations, Hf–sulfate monomers. The bidentate coordination mode of sulfate dominates the dissolved precursors, although it is not found in the structure of the final crystallized product, which instead is comprised of bridging-bidentate sulfate ligation. Neither the PDF patterns nor the Raman spectra show any evidence of the larger oligomers, such as the octadecameric metal clusters, found in similar Zr^{4+} solutions. The oligomeric units found in solution provide insights into possible assembly routes for crystallization. In addition to expanding our understanding of synthesis science this study also reveals differences in the aqueous chemistries between Hf and Zr, two elements with ostensibly very similar chemical behavior.

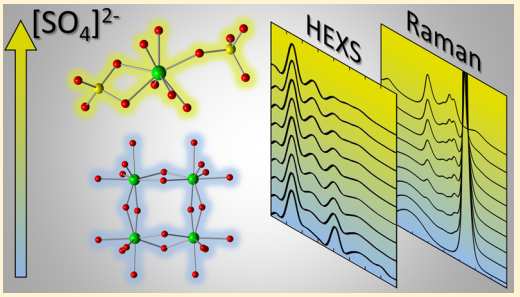

INTRODUCTION

Given the structural complexity and diversity of inorganic materials our understanding remains incomplete of their route from dissolved ions in solution to crystalline materials. The generally accepted classical theory of nucleation[1,2]—involving atom-by-atom cluster growth and Ostwald ripening—overlooks the potential influence of well-defined precursor clusters in solution. This avenue to solid formation has recently been partially addressed through the development of prenucleation concepts,[3] which include the condensation of liquid-like clusters in solution, their subsequent crystallization, and ultimate precipitation. While studying metal correlations in solution, we have found evidence for chemically and structurally distinct clusters with sizes in the 0.5–1.5 nm range.[4−9] While the nanoclusters are too small to produce Bragg diffraction peaks themselves and consequently may be operationally defined as amorphous, they exhibit well-defined correlations that persist and may subsequently condense into solid phases. We present herein evidence for the formation of well-defined small Hf-based clusters in solution and discuss the potential impact of their organization on the materials growth and atomic structures of precipitates. This knowledge bears on our understanding of the mechanisms by which inorganic materials are formed, informs the route to controlled syntheses, and is a step toward the prediction of new phases.

Exemplified by the speciation of tetravalent-metal cations in solution, including Zr^{IV}, Hf^{IV}, Ce^{IV}, and Th^{IV}–Pu^{IV}, the concept of preorganized inorganic clusters in aqueous media is the subject of recent experimental[4,8−11] and computational[12−15] studies. These highly charged ions have long been known to readily undergo hydrolysis and condensation reactions and have been understood to form largely amorphous and ill-defined oligomers.[16,17] Unlike the higher-valent M^{VI} ions such as Mo or W, which are known to form magic-cluster polyoxometalates,[18] it has only recently been understood that the softer tetravalent ions also form monodisperse small clusters, well-defined both chemically and structurally.[19] A variety of polynuclear M^{IV}–oxo/hydroxo clusters ranging in size from simple dimers to large 38-mers have been identified in solution.[19] Our interest centers on directing the composition and structure of the precipitate material through deliberate manipulation of metal speciation and relative cluster stabilities in solution. This approach is built on the assumption of solid formation via preformed-cluster condensation.

Studies of Zr^{IV} aqueous chemistry have revealed a complex solution behavior attributed to hydrolysis and oligomerization reactions that vitiate controlled synthetic approaches. Using this complexity as a starting point, we looked for metal–ion correlations in Zr–sulfate solutions and their relationship to the solids that precipitated.[8] Exploiting information from high-energy X-ray scattering (HEXS) obtained from solution

Received: April 22, 2014
Published: May 28, 2014

   dx.doi.org/10.1021/ic500938k | Inorg. Chem. 2014, 53, 6321−6328

samples we were able to probe the changes in structural correlations across a series of Zr solutions with varying sulfate concentrations. Given the similarity in the ionic radii of tetravalent Hf and Zr,[20] the solution chemistry of two ions should be closely related.[21−23] In the absence of complexing anions, the aqueous solutions of both are dominated by the well-studied tetrameric species $[M_4(OH)_8(H_2O)_{16}]^{8+}$.[10,24] However, a greater tendency for zirconium to polymerize has been detected at low pH.[21,22] More recently, computational studies on monomeric hydrated Hf^{IV} and Zr^{IV} have found that hafnium has a more rigid solvation structure (less exchange) as well as lower hydrolysis tendencies than zirconium.[13,14] Experiments comparing solution correlations of these two ions were undertaken to enlighten the discourse on the mechanisms of inorganic materials formation as well as providing insights into the challenges associated with controlling their solution chemistry.

The sulfate ligand is particularly useful for investigating metal−oxo/hydroxo clusters. Being a strongly coordinating ligand that bridges metal ions, it promotes oligomerization[24,25] and stabilizes clusters by protecting their surfaces.[26,27] For Hf and Zr, the clusters crystallized from sulfuric acid solutions have included rare structures that have not been found for other tetravalent cations. Examples include a flat pentagonal hexamer,[28] a nonamer,[27] and 18-mers.[26,29] These uncommon clusters may have important structure-directing effects on the materials that precipitate under similar solution conditions. Understanding their solution behavior, as well as the role of the sulfate ligand in their formation, is valuable for the synthesis of functional Hf and Zr materials using methods such as aqueous sol−gel synthesis.[30−34] The aim of this work is to observe the influence of sulfate on the Hf species in solution and to gain insights into the building units that form prior to crystallization. In addition, the experimentally demonstrated differences in the aqueous chemistries between Hf^{4+} and Zr^{4+} are described and discussed.

EXPERIMENTAL METHODS

Solution Preparation. A series of nine aqueous acidic solutions containing 0.4 molal (m) Hf with varying perchlorate and sulfate concentrations, added in the form of $HClO_4$ and H_2SO_4, were prepared. The series covered the concentration range of 4.00−0.00 m perchlorate, whereas the sulfate range was 0.00−2.00 m, such that 2 equiv of $HClO_4$ were replaced by 1 equiv of H_2SO_4. This was done to minimize variations in pH and ionic strength across the series. Previous work on a similar Zr series showed no evidence of perchlorate interference with trends established in the studies.[8] Samples were made in 0.50 m steps in perchlorate and 0.25 m steps in sulfate. The samples were prepared by dissolving $HfOCl_2{\cdot}8H_2O$ (Alfa Aesar, ≥98%) with appropriate amounts of deionized water (18.2 MΩ·cm), concentrated $HClO_4$ (Fisher Scientific, Optima), and concentrated H_2SO_4 (Fisher Scientific, Optima) solutions. Background samples were prepared in a similar manner but with $HfOCl_2{\cdot}8H_2O$ replaced by the appropriate amount of concentrated HCl.

Crystal Growth of $[Hf_4(OH)_8(H_2O)_{16}]Cl_8{\cdot}12H_2O$ (1). Large crystals of the starting material (**1**), suitable for single-crystal X-ray diffraction, were grown to accurately determine its crystal structure for direct comparison with solution correlations. $HfOCl_2{\cdot}8H_2O$ (204.8 mg, 0.5 mmol) and HCl (214.5 mg, 34%, 2 mmol) were dissolved in water (777.4 mg) to give a total water mass of 1000 mg and concentrations of 0.5 and 2 m, respectively. The solution was allowed to evaporate slowly at room temperature in an open vial. Large needle-like crystals of **1** formed after 1−2 weeks of slow evaporation.

Synthesis of $Hf(SO_4)_2{\cdot}4H_2O$ (2). $HfOCl_2{\cdot}8H_2O$ (327.6 mg, 0.8 mmol) and H_2SO_4 (1858.3 mg, 95%, 18 mmol) were dissolved in water (1777 mg) to give a total water mass of 2000 mg and concentrations of 0.4 and 9 m, respectively. After standing the solution in a closed vial for 1 week, large prismatic crystals suitable for single-crystal X-ray diffraction were obtained.

High-Energy X-ray Scattering. Data were collected in transmission geometry on the series of Hf−perchlorate/sulfate solutions along with the background solutions and empty holders. Experiments were carried out at the Advanced Photon Source (APS), Argonne National Laboratory, on beamline 11-ID-B using an incident-beam energy of 91 keV (0.13702 Å). HEXS data were acquired at room temperature using an amorphous, silicon, flat-panel X-ray detector. It was mounted in a static position ($2\theta = 0°$) at two different sample−detector distances, allowing a data collection over a range in momentum transfer space of $Q = 0.2−28$ $Å^{-1}$.[35,36] The data were treated as described previously.[8] Spectra were corrected for background scattering (by subtracting an empty sample holder) and polarization; they were subsequently normalized to a cross section per formula unit. Correlations not involving Hf were eliminated by subtracting data obtained from background solutions, as described previously.[35,36]

Raman Spectroscopy. Raman spectra were collected on the Hf solution series using a Renishaw inVia Raman Microscope with an excitation wavelength of 532 nm at 100% laser power. Each spectrum consists of the summation of 100 acquisitions. Raman spectra were also collected on crystals of compounds **1** and **2**. For both samples, multiple crystals were examined to confirm sample homogeneity and phase purity. The 532 nm laser was used, but the power was dropped to 50%; only 10 acquisitions were acquired.

RESULTS AND DISCUSSION

Given general similarities in the experimental protocols employed for this study and our previous work on Zr, designed because of the expected similarities in the behavior of Hf and Zr, the results of this investigation are compared directly with those from our published Zr−sulfate study.[8] Whereas both HEXS and Raman data are very similar when comparing the Hf and Zr solutions, some unexpected differences were found as the sulfate ligand was introduced. As a foundation for interpreting correlations observed in solution, we begin with a description of the solid-state structures obtained from the analysis of single-crystal precipitates.

Solid-State Structures. Minimal metrical information from two solid-state structures, crystallized at room temperature from acidic Hf−sulfate−chloride solutions, is included herein; for further details see the Supporting Information. Unlike the Zr solution series,[8] the 18-mer cluster does not crystallize at room temperature.

Compound **1**, $[Hf_4(OH)_8(H_2O)_{16}]Cl_8{\cdot}12H_2O$, commonly written as $HfOCl_2{\cdot}8H_2O$, is the starting material, which recrystallizes when no sulfate is present. Crystallizing in the tetragonal space group $P\bar{4}2_1c$, it contains isolated tetrameric $[Hf_4(OH)_8(H_2O)_{16}]^{8+}$ units that are interlinked through hydrogen bonding with Cl^- and H_2O in the voids. Within the tetramer, each Hf is bridged to the next by two μ_2-OH groups forming a square arrangement (see Figure 1). The structure presented herein clarifies a minor discrepancy between previously published $ZrOCl_2$ and $Hf/ZrOCl_2$ reports concerning the location of the Cl^- ions.[10,24]

At high sulfuric acid concentrations compound **2**, the hydrated sulfate salt $Hf(SO_4)_2{\cdot}4H_2O$, is obtained. It crystallizes in the orthorhombic space group *Fddd* and is isostructural with $Zr(SO_4)_2{\cdot}4H_2O$.[37] The space group and unit cell parameters of this compound were previously confirmed using powder X-ray diffraction.[38] Compound **2** represents the end point of the sulfate addition to the Hf^{4+} solution with four bridging μ_2-

dx.doi.org/10.1021/ic500938k | Inorg. Chem. 2014, 53, 6321−6328

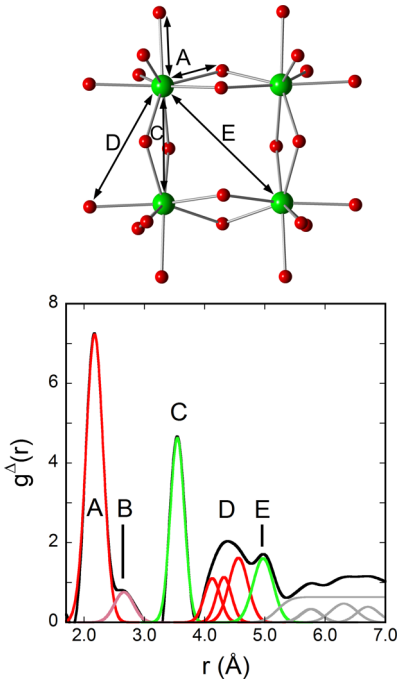

Figure 1. (top) A tetrameric $[Hf_4(OH)_8(H_2O)_{16}]^{8+}$ unit from the crystal structure of compound **1**. Hf atoms are represented by green spheres. Oxygen atoms, belonging either to terminal H_2O ligands or bridging μ_2-OH ligands, are shown in red. Representative distances are labeled with corresponding assignments from the solution PDF pattern. (bottom) PDF pattern obtained from HEXS of sulfate-free solution. The data is shown in black. The Gaussian peaks represent fits to the data and are color-coded according to the proposed correlation assignments: O (red), H (pink), Hf (green), and unassigned (gray).

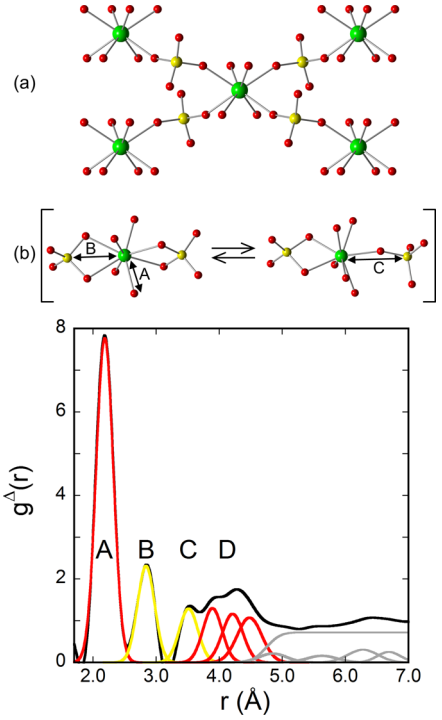

Figure 2. (top) (a) A section of the crystal structure of compound **2**. (b) Possible equilibrated species in 2 m sulfate solution. Atoms are colored as follows: Hf (green), S (yellow), and O (red). (bottom) PDF obtained from HEXS of 2 m sulfate solution. The data are shown in black.

sulfates bonded to each hafnium in a monodentate configuration. Each sulfate in turn bridges two hafnium centers, creating layers of hafnium sulfate. The layers are held together by hydrogen bonding interactions. A fragment of a layer in this structure is illustrated in Figure 2.

Solution HEXS. *Sulfate-Free Solution.* We start by examining the solutions that relate closely to compounds **1** and **2**, namely, the sulfate-free and most-concentrated sulfate solutions in the series (i.e., the Hf solution in 4 m perchloric acid vs that in 2 m sulfuric acid, respectively). Peaks attributed to Hf correlations were observed out to distances of about 7 Å, but intensities were only analyzed out to the second coordination sphere owing to increasing solution disorder that markedly increases at longer distances.[36] The PDF pattern for the 4 m perchloric acid, sulfate-free solution is shown in Figure 1, with suggested peak assignments provided in Table 1. Because the data are presented as a difference PDF, all peaks are attributed to correlations with Hf, specifically Hf–Hf, Hf-solvent, or Hf–other solute correlations. On the basis of our complementary Zr studies done in the absence of perchlorate we argue that Hf correlations are unlikely with the weakly coordinating perchlorate anion. The first two peaks, A and B at 2.17 and 2.66 Å, are assigned to 7.5(4) O and about 10 H atoms from coordinating H_2O or OH^-. These assignments are consistent with the first coordination sphere of Hf in the solid tetramer (**1**). Metal–H correlations have been previously observed, assigned both based on the M–H distance and the peak intensity, notably with relation to an M–O (water) intensity, where they are expected to be about 25% of the latter.[7,39]

Also present in the solution PDF is a peak at 3.55(2) Å, the same distance as that observed between adjacent dihydroxo-bridged Hf in the tetramer (**1**). Whereas two such adjacent Hf interactions are expected in the tetramer, the peak intensity in solution corresponds to 2.3(1) Hf–Hf interactions. Information from **1** provides little insight into the source of the extra peak intensity over the two interactions expected at that distance for the tetramer, the Hf–opposite O interaction (D) at 3.96 and 3.99 Å being far enough away that they should be at least partially resolvable. Hf–second coordination Cl^-, should they occur, are expected to be in the range of 4.57–5.00 Å. Even the Th^{IV} dihydroxy-bridged dimer, which includes a Cl^- in the inner coordination sphere of the solid, shows no evidence of Th–Cl inner-sphere complexation in solution.[40] The most plausible cause for the excess scattering in the 3.55 Å peak is additional adjacent Hf–Hf correlations, which point to the presence of clusters larger than tetramers. Because the peak represents the average number of correlations, this interpretation requires an average cluster size larger than a tetramer, although the tetrameric unit may still dominate the Hf solution speciation. Similar findings were reported in our Zr HEXS studies, even for the sulfate-free sample. These results are also consistent with recently reported electrospray ionization mass spectrometry and small-angle X-ray scattering (SAXS) studies on Hf–sulfate, which were reported to be consistent with an octamer composed of two linearly joined tetramers.[41] Previous SAXS studies proposed that the tetramer is in equilibrium with an octamer composed of two stacked tetramers.[42]

Octahedral hexamers may also be present in equilibrium with the tetramer. However, the correlation observed in solution HEXS data at 5.54 Å for Zr[8] and Th,[9] attributed to the distal metal–metal interaction in the hexamer and considered

dx.doi.org/10.1021/ic500938k | Inorg. Chem. 2014, 53, 6321–6328

Table 1. Assignment of Fitted Peaks for the PDF Pattern of the Sulfate-Free Solution Shown in Figure 1. Comparison with the Actual Hf-Correlations Found in Compound 1 Are Provided

HEXS PDF peaks				comparison: Hf distances in compound 1		
peak	intensity (electrons)	center (Å)	suggested assignment	distance (Å)	moieties	atoms
A	60(3)	2.17	7.5(4) O	2.10−2.31	4 OH, 4 H_2O	8 O
B	10(4)	2.66	10 H		4 OH, 4 H_2O	12 H
C	83(3)	3.55	2.3(1) Hf*	3.54	2 Hf (adj)	2 Hf
D	(30 + 32)	4.13		3.96−3.99	2 OH (diag)	10 O
		4.32		4.23−4.24	2 H_2O (adj)	
				4.55−4.66	2 OH (diag), 2 H_2O (adj)	
	65(5)	4.56	water/Cl	4.79−4.80	2 H_2O (adj)	
E	81(6)	4.97	Hf[a] (Cl,H_2O)	5.00	1 Hf (diag)	1 Hf
		5.77		5.73−5.75	2 H_2O (adj)	2 O
		6.31		6.24−6.30	2 H_2O (diag)	2 O
		6.71		6.78−6.79	2 H_2O (diag)	2 O

[a]Correlations involving atoms of the same element contribute only 1/2 of their electron count (i.e., one Hf−Hf interaction = 36 electrons).[36]

Table 2. Assignment of Fitted Peaks for the PDF Pattern of the Sulfate-Rich Solution Shown in Figure 2. Related Hf-Correlations within a Single Layer in Compound 2 Are Shown For Comparison

HEXS PDF peaks				comparison: Hf distances in compound 2		
peak	intensity (electrons)	center (Å)	suggested assignment	distance (Å)	moieties	atoms
A	56(4)	2.18	7.0(5) O	2.17	4 SO_4 (m), 4 H_2O	8 O
B	19(3)	2.84	1 SO_4 (b)	2.73−2.74	4 H_2O	8 H
C	33(3)	3.51	2 SO_4 (m)	3.53	4 SO_4 (m)	4 S
D	(33 + 36)(5)	3.89	4 O (SO_4, m)	3.88	4 SO_4 (m, 1 O each)	4 O
		4.21	4 O (SO_4, m)	4.35	4 SO_4 (m, 1 O each)	4 O
	37(5)	4.48	4 O (SO_4, m)	4.41	4 SO_4 (m, 1 O each)	4 O
		4.85	H_2O (outer sphere)			
		5.63				
		6.28				
		6.69	Hf−Hf[a]	6.42	4 Hf (S-bridged)	4 Hf

[a]Correlations involving atoms of the same element contribute only 1/2 of their electron count (i.e., one Hf−Hf interaction = 36 electrons),[36] b = bidentate, m = mondentate.

definitive for its presence, is not discernible in the Hf data, which may simply reflect a reduced relative concentration of higher-order species, as indicated by the peak intensities of the adjacent M−M interactions.

Oligomers larger than the tetramer have been reported as isolated units in solid-state structures, obtained as precipitates from aqueous solution. Hexameric structures $[M_6(OH)_4O_4]^{12+}$ appear to be particularly prevalent,[19] stabilized with a variety of anions, including carboxylic acids, sulfate, and selenate with M^{IV} = Zr,[43] Ce,[44] Th,[45] U,[46−48] and Pu.[49] A nonomeric Hf oxyhydroxide, stabilized as the sulfate, was recently reported.[27] Larger structures, including the oxyhydroxide 18-mer, have been isolated for Zr[26] and Hf.[29] Even larger clusters including the 38-mer, an oxide nanoparticle, have been isolated for U[48] and Pu,[5] the latter obtained from chloride solution, but they have not currently been reported for either Hf or Zr.

2 m Sulfate Solution. The HEXS PDF pattern for the sulfate-rich solution is shown in Figure 2 with details of the peak assignments provided in Table 2. In contrast with the sulfate-free solution results, the correlations present in the sulfate-rich solution differ considerably from the distances observed in the corresponding solid precipitate, compound **2**. The first peak at 2.18 Å is assigned to 7.0(5) O in the first-coordination sphere around Hf. This coordination number is lower than that seen in the tetramer (eight-coordinate) but finds precedent in a variety of solid-state oxides,[50] sulfates,[51,52] and clusters.[28,29] The two coordination environments may be in equilibrium in solution, lowering the average electron count.

The PDF resolution is not sufficient to differentiate O atoms belonging to sulfate, water, or bridging-hydroxide ligands.[53] However, longer-*r* correlation peaks provide insight in this regard, such as peak B centered at 2.84 Å, which has shifted to slightly longer *r* from the second peak in the sulfate-free sample where it was attributed to Hf−proton interactions. A comparison with the correlations found in **2** reveals that there are no Hf correlations corresponding to this distance in the solid. Instead, the position and high electron count of this correlation peak are indicative of bidentate (chelating, η_2) sulfate ligands coordination to Hf. Although not present in compound **2**, the bidentate mode has been observed in Hf and Zr sulfate salts, especially those containing charge-balancing monovalent cations (alkali metal or ammonium).[54−58] The peak intensity indicates that there are slightly less than two such interactions on average per Hf.

The region of the PDF centered at about 3.5 Å, indicative of Hf−Hf interactions, is markedly different in the sulfate-derived pattern shown in Figure 2 from that observed in Figure 1 for the sulfate-free sample. The peak observed in the sulfate-rich case is slightly shifted to lower *r* and is decreased significantly in intensity. With the assistance of the trends established by the intermediate sulfate samples and the structure of **2**, this peak is assigned to about 1.6 sulfate coordinating to Hf in a monodentate fashion. In the solid state these sulfates bridge

dx.doi.org/10.1021/ic500938k | Inorg. Chem. 2014, 53, 6321−6328

two Hf, separated by a distance of 6.42 Å. There is some evidence of such an interaction in solution, at 6.69 Å at high sulfate concentrations.

Combining these results gives us a perspective on the first-coordination sphere of Hf in this sulfate-rich solution. Of the seven coordinating O atoms, on average four are associated with the two bidentate sulfates and 1.6 with the monodentate sulfate, leaving about 1.4 O from water. In the unlikely absence of water or sulfate protonation, the complex $Hf(SO_4)_2(SO_4)_{1,6}(H_2O)_{1.4}$ would be anionic. The bulkiness of the coordination environment may account, at least in part, for the reduced Hf coordination number over that seen for the tetramer.

The three peaks seen in the PDF at 3.89–4.48 Å are attributed to the terminal oxygen atoms of the sulfate groups. Accurate electron counts are vitiated in this region of the pattern because of pattern resolution and because of the onset of significant scattering background resulting from the amorphous nature of solution samples. Nevertheless, peak positions remain reliable and can be used to support lower-*r* assignments. The peak at 3.89 Å is thus exclusively assigned to terminal oxygens on the bidentate sulfates based on the typical distance found in solid-state compounds.[54−58] There is clearly no strong evidence for a Hf–Hf diagonal correlation at ∼5 Å to be attributed to the tetramer, whereas a weak peak at 4.85 Å is likely to be an outer-sphere water.

Overall, when compared with the sulfate-rich analogue in the Zr series,[8] the Hf sulfate-rich solution has very similar correlations. The various indicators taken from this PDF pattern suggest that the solution species are predominately monomeric Hf coordinated by bidentate sulfate, monodentate sulfate, and water molecules. With regards to the sulfate, the dominant bidentate ligation may be in equilibrium with the monodentate alternative, since the corresponding precipitate (compound **2**) is fully monodentate (see Figure 2). The formation of a variety of sulfate salts from aqueous solution that possess various combinations of monodentate and bidentate sulfates further suggests similar energetics between the two binding modes and hence a possible equilibrium between the two. Some monodentate sulfate may bridge two Hf centers together in this solution. OH-bridging, however, seems minimal or absent. The main difference that stands out is that the Zr species appear to have three bidentate sulfates. There is no evidence that either metal has a higher degree of oligomerization in these sulfate-rich solutions; monomeric species appear to dominate both.

Solution Series with Varying Sulfate Concentration. HEXS data from the sulfate-free and sulfate-rich solutions, together with structures from the precipitating solids, suggest that the Hf solution speciation changes smoothly as a function of sulfate concentration. The PDF plots and the low *Q* scattering data for the entire Hf solution series are shown in Figure 3. Inspection of the PDFs reveals, as a general observation, that the correlation intensities are shifting to lower *r* with increasing sulfate concentration. The diagonal Hf–Hf correlation, which occurs at 4.97 Å in the sulfate-free solution, disappears at the low $[SO_4]^{2-}$. In addition, the peak at 3.55 Å, attributed to adjacent Hf–Hf correlations in the sulfate-free solution, is replaced by correlations arising from monodentate-bound sulfur.

Inspection of the low-Q scattering data in Figure 3 reveals a gradually decreasing intensity at low angle as the sulfate concentration rises, consistent with the decreasing intensity of

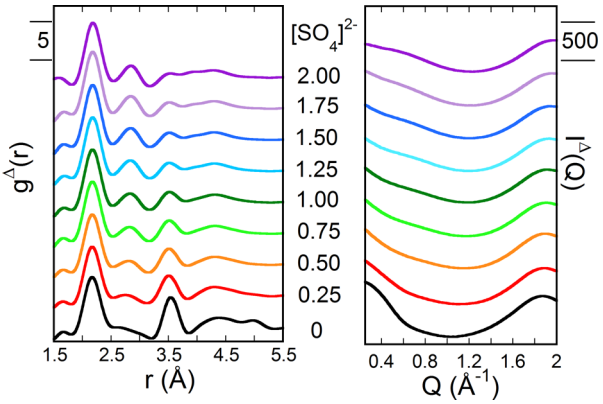

Figure 3. (left) PDF patterns Fourier-transformed from background subtracted HEXS data of the Hf solution series as a function of sulfate concentration. (right) Background-subtracted, low-Q scattering data over the same series.

the peaks at higher *r* in the PDF patterns. This behavior is consistent with a decrease in average cluster size and a break up of tetramers (and larger clusters) present in the sulfate-free solution into smaller species upon the addition of sulfate. In contrast, for analogous Zr samples nonlinear trends were observed in the PDF peaks. Most notably, the 3.5 Å peak, attributed to adjacent Zr–Zr correlation, intensifies as the sulfate ligand is introduced, reaching a maximum at $[SO_4]^{2-}$ = 0.5 m before diminishing at higher sulfate concentrations. The Zr results were interpreted as the formation of large oligomers, possibly including species as large as 18-mers, in solutions with low $[SO_4]^{2-}$; the addition of even more sulfate breaks them apart into smaller species. The low-Q scattering data for Zr revealed an increase in average cluster size initially as sulfate is introduced, followed by a gradual decrease as $[SO_4]^{2-}$ rises. For Hf, however, these cluster-growth events at low $[SO_4]^{2-}$ are not detected. The observation that Hf, in comparison to Zr, resists the formation of larger clusters such as the 18-mer is consistent with recently reported SAXS results[41] and supports the experimental[21,22] and computational[13,14] studies reporting that Hf polymerizes less readily in aqueous solution than does Zr.

Contrasting the trend to decreasing correlations at longer *r* is the shorter-distance correlation behavior. Although the scattering intensity from the Hf nearest neighbors at 2.18 Å may decrease slightly across the series, the peak at 2.84 Å, which first appears at the lowest sulfate concentration, grows with increasing concentration of $[SO_4]^{2-}$. It is attributed to bidentate sulfate ligation to Hf. The growth of the bidentate sulfate peak correlates with the decline of the two Hf–Hf correlations in the tetramer. The bidentate sulfate grows gradually at low sulfate concentrations and levels off at around $[SO_4]^{2-}$ = 1.25 m. Meanwhile, the adjacent Hf–Hf correlation at 3.55 Å, whose position coincides with the S from monodentate sulfate, decreases gradually throughout. The gradual decline of this peak indicates that the adjacent Hf–Hf correlation remains dominant at low sulfate concentration, decreasing gradually as sulfate is added. The drop in the diagonal Hf–Hf correlation, at 4.97 Å, is more dramatic. At $[SO_4]^{2-}$ > 0.5 m, the electron contribution to this peak is essentially negligible, revealing that the tetrameric $[Hf_4(OH)_8(H_2O)_{16}]^{8+}$ units do not survive in the presence of sulfate. However, OH-bridged Hf dimers or chains of dimers appear to persist at low $[SO_4]^{2-}$ and perhaps even approaching

dx.doi.org/10.1021/ic500938k | *Inorg. Chem.* 2014, 53, 6321−6328

$[SO_4]^{2-}$ = 2 m. The concentration of these species, and their average size, decreases as the sulfate concentration rises.

Raman Spectroscopy. Raman spectra for the Hf solution series are displayed in Figure 4. The positions of the Raman

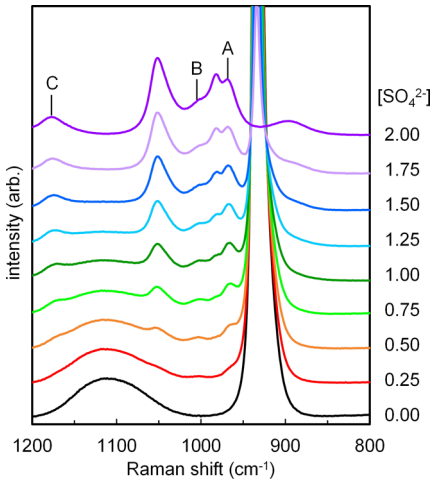

Figure 4. Raman spectra of the Hf solution series as a function of sulfate concentration.

active peaks belonging to perchlorate and sulfate anions in aqueous solution are well-documented.[8,59−61] As the series progresses from the sulfate-free to the sulfate-rich solution, the perchlorate peaks at 934 and 1115 cm^{-1} decrease in intensity, while those of the sulfate at 983 and 1052 cm^{-1} emerge and intensify. These peaks are present in the background solutions and behave identically along the series, meaning they generally lack the involvement of Hf species. However, there are three peaks that appear upon sulfate addition that are absent from the background solutions, indicating they belong to vibrational modes resulting from species where sulfate is coordinated to (or interacting with) Hf in solution. These peaks at 967, 1017, and 1180 cm^{-1} (labeled A, B, and C, respectively, in Figure 4), are difficult to assign due to the complexity of the solution speciation. In accordance with the HEXS data, the intensities of A and C increase gradually throughout the series as sulfate is added. The B peak, however, is weak and shows little change after the initial introduction of sulfate. In contrast, the analogous Zr work found that the B peak (at 1017 cm^{-1}) exhibited non-incremental change as the sulfate ligand is introduced.[8] This peak grew significantly at low $[SO_4]^{2-}$, reaching a maximum at $[SO_4]^{2-}$ = 0.5 m, before fading away at higher sulfate concentrations. This behavior led to the interpretation that the 1017 cm^{-1} peak is related to the growth of a large cluster, possibly the 18-mer. The fact that this peak appears much less pronounced for Hf further supports the assignment from the Zr series, since no 18-mer can be crystallized at room temperature with Hf, and no evidence was found of an increase in the average cluster size as sulfate was added.[41] The solution Raman spectra collected were dominated by perchlorate and sulfate peaks. The Raman spectra acquired on crystals of compound **1** revealed two peaks at 472 and 589 cm^{-1} that can be assigned to either the Hf−O(H)−Hf or Hf−$O(H_2)$ vibrations in the tetramer (see Supporting Information). In solution, however, these peaks are weak and buried under those of the tetrahedral anions $[ClO_4]^-$ and $[SO_4]^{2-}$. When replacing the tetrahedral anions with Cl^- in solution (using 4 m HCl), the two modes originating from the tetramer were detected.

Suggested Solution Speciation Scheme. Incorporating all the findings from the HEXS and solid-state structural data into a cohesive picture, a scheme for the Hf speciation as a function of solution sulfate is presented in Figure 5. Using these

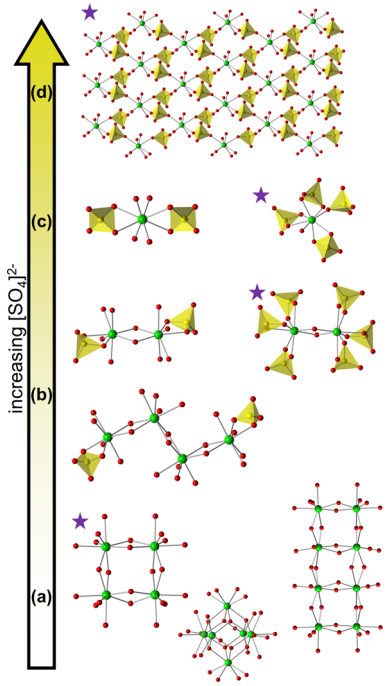

Figure 5. A series of possible Hf species as a function of sulfate concentration. (a) Hydroxo-bridged species, (b) hydroxo-bridged, sulfate-capped chains and dimers, (c) monomers, (d) extended layers (crystallization). The starred species represent fragments that have been found in the solid state in the present work and elsewhere.[57,58]

results it is argued that increasing the sulfate concentration results in the replacement of the Hf dihydroxo-bridged linkages, including the tetrameric, dimeric, and other Hf−Hf species, with bidentate sulfate coordination to Hf. Given that a high concentration of the sulfate anion is required to crystallize compound **2**, we may regard the monomeric Hf species (found in the 2 m sulfate solution) known to be coordinated by bidentate sulfates to be the dominant solution species serving as a building unit (precursor) to the solid phase. An idealized scheme for the opening and break up of dihydroxo-bridged tetramer can be proposed based on these findings (see left column in Figure 5). Without necessarily varying the number of water molecules coordinated to each hafnium center (four), the sulfate ion can be viewed as a substituting ligand for the bridging hydroxyl group on each hafnium.[62,63] Each double hydroxyl bridge can be broken and displaced by two bidentate sulfates each coordinating to one of the two Hf atoms. It is argued that the process initially favors the opening of the tetramer and other oligomers forming chains, which then break into dimers and finally monomers. The latter species can be seen as precursor building units for compound **2**, whereby the layers are constructed by the opening of each bidentate sulfate to form a bridge to the next Hf atom in the layer. In this idealized scheme, an equilibrium between the bidentate and monodentate binding modes allows for the transition from the building units to condensed layers.

dx.doi.org/10.1021/ic500938k | Inorg. Chem. 2014, 53, 6321−6328

CONCLUSION

The hafnium solution chemistry is dominated by the presence of Hf^{4+} oligomers in the absence of strong complexing anions, such as sulfate, even at very low pH. Similar to Zr^{4+} chemistry under related conditions, PDF patterns, generated from HEXS data, are consistent with the presence in solution of tetrameric $[Hf_4(OH)_8(H_2O)_{16}]^{8+}$ units that constitute the primary phase that precipitates. Also similar to Zr^{4+} results, the intensity of the PDF peak attributable to adjacent dihydroxy-bridged Hf correlations is higher than can be rationalized by the sole presence of the tetrameric $[Hf_4(OH)_8(H_2O)_{16}]^{8+}$ unit and, thus, indicates the concurrent presence of higher-order oligomers. An equilibrium is suggested between these different species that rationalizes the quantitative precipitation of the Hf-tetramer. The same perspective can be taken on a Hf^{4+} solution rich in sulfate, wherein the solution speciation shows a predominance of bidentate-coordinated Hf, and yet the solid that precipitates has sulfates bridging two different Hf. There is some evidence of the latter species in the solution from which the precipitate forms. This suggests an equilibrium between monodentate and bidentate sulfate ligation.

The subtle differences in the Hf solution behavior observed here and the previous study on similar Zr solutions[8] may provide avenues for probing their origins. For example, calculations have suggested that monomeric hydrated Hf^{4+} has a more rigid solvation structure (less exchange) than does Zr^{4+}.[13,14]

Like other small, highly-charged ions, the aqueous chemistry of Hf^{4+} is dominated by hydrolysis and subsequent condensation reactions. The result is the possibility for the simultaneous presence of multiple species, including metal hydroxide, hydrous oxides, or oxidic oligomers, which may or may not exist in equilibria. Overall, their presence may significantly impact a metal ion's relative energetics, reactivity, and solubility with an influence that can change as solution conditions change through these equilibria, thus adding to the complexity of exhibited chemistry. The results of this study on Hf in acidic solutions with varying sulfate concentrations constitute the first steps in unraveling this complex chemical system. They provide a window into the equilibria that are present and how they may be controlled to harness the chemistry and direct targeted syntheses.

ASSOCIATED CONTENT

Supporting Information

Crystallographic information, X-ray structure determination information, ORTEP illustrations and structural details for compounds **1** and **2**. Additional solution and solid-state Raman spectra. This material is available free of charge via the Internet at http://pubs.acs.org. Crystallographic data have also been deposited with the Inorganic Crystal Structure Database (ICSD) and may be obtained at http://icsd.fiz-karlsruhe.de by referencing Nos. 427624 (compound **1**) and 427625 (compound **2**).

AUTHOR INFORMATION

Corresponding Author

*E-mail: LS@anl.gov.

Notes

The authors declare no competing financial interest.

ACKNOWLEDGMENTS

This work is supported by the U.S. Department of Energy, Office of Basic Energy Sciences under Contract DE-AC02-06CH11357. The Advanced Photon Source, used to obtain the HEXS data described in this study, is supported by the U.S. DOE, OBES, Materials Sciences under the same contract number.

REFERENCES

(1) Stumm, W.; Morgan, J. J. *Aquatic chemistry: Chemical equilibria and rates in natural waters,* 3rd ed.; Wiley-Interscience: Hoboken, NJ, 1996.
(2) Debenedetti, P. G. *Metastable liquids: Concepts and principles;* Princeton University Press: Princeton, NJ, 1996.
(3) Gebauer, D.; Kellermeier, M.; Gale, J. D.; Bergström, L.; Cölfen, H. *Chem. Soc. Rev.* **2014**, *43*, 2348.
(4) Soderholm, L.; Skanthakumar, S.; Gorman-Lewis, D.; Jensen, M. P.; Nagy, K. L. *Geochim. Cosmochim. Acta* **2008**, *72*, 140.
(5) Soderholm, L.; Almond, P. M.; Skanthakumar, S.; Wilson, R. E.; Burns, P. C. *Angew. Chem., Int. Ed.* **2008**, *47*, 298.
(6) Skanthakumar, S.; Antonio, M. R.; Soderholm, L. *Inorg. Chem.* **2008**, *47*, 4591.
(7) Soderholm, L.; Skanthakumar, S.; Wilson, R. E. J. *Phys. Chem. A* **2009**, *113*, 6391.
(8) Hu, Y.-J.; Knope, K. E.; Skanthakumar, S.; Kanatzidis, M. G.; Mitchell, J. F.; Soderholm, L. *J. Am. Chem. Soc.* **2013**, *135*, 14240.
(9) Hu, Y.-J.; Knope, K. E.; Skanthakumar, S.; Soderholm, L. *Eur. J. Inorg. Chem.* **2013**, *2013*, 4159.
(10) Hagfeldt, C.; Kessler, V.; Persson, I. *Dalton Trans.* **2004**, 2142.
(11) Hennig, C.; Schmeide, K.; Brendler, V.; Moll, H.; Tsushima, S.; Scheinost, A. C. *Inorg. Chem.* **2007**, *46*, 5882.
(12) Lutz, O. M. D.; Hofer, T. S.; Randolf, B. R.; Weiss, A. K. H.; Rode, B. M. *Inorg. Chem.* **2012**, *51*, 6746.
(13) Messner, C. B.; Hofer, T. S.; Randolf, B. R.; Rode, B. M. *Chem. Phys. Lett.* **2011**, *501*, 292.
(14) Messner, C. B.; Hofer, T. S.; Randolf, B. R.; Rode, B. M. *Phys. Chem. Chem. Phys.* **2011**, *13*, 224.
(15) Vallet, V.; Macak, P.; Wahlgren, U.; Grenthe, I. *Theor. Chem. Acc.* **2006**, *115*, 145.
(16) Baes, C. F.; Mesmer, R. E. *The hydrolysis of cations;* Wiley: New York, 1976.
(17) Henry, M.; Jolivet, J. P.; Livage, J. In *Chemistry, spectroscopy and applications of sol-gel glasses;* Reisfeld, R., Jørgensen, C. K., Eds.; Springer-Verlag: Berlin, Germany, 1992; p 153.
(18) Mueller, A.; Peters, F.; Pope, M. T. *Chem. Rev.* **1998**, *98*, 239–271.
(19) Knope, K. E.; Soderholm, L. *Chem. Rev.* **2013**, *113*, 944.
(20) Shannon, R. D. *Acta Crystallogr., Sect. A* **1976**, *32*, 751.
(21) Johnson, J. S.; Kraus, K. A. *J. Am. Chem. Soc.* **1956**, *78*, 3937.
(22) Muha, G. M.; Vaughan, P. a. *J. Chem. Phys.* **1960**, *33*, 194.
(23) Åberg, M. *Acta Chem. Scand., Ser. B* **1977**, *31*, 171.
(24) Clearfield, A. *Rev. Pure Appl. Chem.* **1964**, *14*, 91.
(25) Matijevic, E. *Acc. Chem. Res.* **1981**, *14*, 22.
(26) Squattrito, P. J.; Rudolf, P. R.; Clearfield, A. *Inorg. Chem.* **1987**, *26*, 4240.
(27) Kalaji, A.; Soderholm, L. *Chem. Commun.* **2014**, *50*, 997.
(28) Kuznetsov, V. Y.; Dikareva, L. M.; Rogachev, D. L.; Porai-Koshits, M. A. *J. Struct. Chem.* **1985**, *26*, 923.
(29) Mark, W.; Hansson, M. *Acta Crystallogr., Sect. B* **1975**, *31*, 1101.
(30) Alves Rosa, M. A.; Sanhueza, C. S. S.; Santilli, C. V.; Pulcinelli, S. H.; Briois, V. *J. Phys. Chem. B* **2008**, *112*, 9006.
(31) Anderson, J. T.; Munsee, C. L.; Hung, C. M.; Phung, T. M.; Herman, G. S.; Johnson, D. C.; Wager, J. F.; Keszler, D. A. *Adv. Funct. Mater.* **2007**, *17*, 2117.
(32) Kickelbick, G.; Wiede, P.; Schubert, U. *Inorg. Chim. Acta* **1999**, *284*, 1.
(33) Chiavacci, L. A.; Pulcinelli, S. H.; Santilli, C. V.; Briois, V. *Chem. Mater.* **1998**, *10*, 986.

(34) Chiavacci, L. A.; Santilli, C. V.; Pulcinelli, S. H.; Bourgaux, C.; Briois, V. *Chem. Mater.* **2004**, *16*, 3995.
(35) Soderholm, L.; Skanthakumar, S.; Neuefeind, J. *Anal. Bioanal. Chem.* **2005**, *383*, 48.
(36) Skanthakumar, S.; Soderholm, L. *Mater. Res. Soc. Symp. Proc.* **2006**, *893*, 411.
(37) Singer, J.; Cromer, D. T. *Acta Crystallogr.* **1959**, *12*, 719.
(38) Bear, I. J.; Mumme, W. G. *J. Inorg. Nucl. Chem.* **1970**, *32*, 1159.
(39) Soderholm, L.; Skanthakumar, S.; Wilson, R. E. J. *Phys. Chem. A* **2011**, *115*, 4959.
(40) Wilson, R. E.; Skanthakumar, S.; Sigmon, G.; Burns, P. C.; Soderholm, L. *Inorg. Chem.* **2007**, *46*, 2368.
(41) Ruther, R. E.; Baker, B. M.; Son, J.-H.; Casey, W. H.; Nyman, M. *Inorg. Chem.* **2014**, *53*, 4234.
(42) Singhal, A.; Toth, L. M.; Lin, J. S.; Affholter, K. *J. Am. Chem. Soc.* **1996**, *118*, 11529.
(43) Pan, L.; Heddy, R.; Li, J.; Zheng, C.; Huang, X.-Y.; Tang, X.; Kilpatrick, L. *Inorg. Chem.* **2008**, *47*, 5537.
(44) Lundgren, G. *Ark. Kemi* **1956**, *10*, 183.
(45) Knope, K. E.; Wilson, R. E.; Vasiliu, M.; Dixon, D. A.; Soderholm, L. *Inorg. Chem.* **2011**, *50*, 9696.
(46) Takao, S.; Takao, K.; Kraus, W.; Emmerling, F.; Scheinost, A. C.; Bernhard, G.; Hennig, C. *Eur. J. Inorg. Chem.* **2009**, 4771.
(47) Falaise, C.; Volkringer, C.; Loiseau, T. *Cryst. Growth Des.* **2013**, *13*, 3225.
(48) Loiseau, T.; Mihalcea, I.; Henry, N.; Volkringer, C. *Coord. Chem. Rev.* **2014**, *266*−*267*, 69.
(49) Knope, K. E.; Soderholm, L. *Inorg. Chem.* **2013**, *52*, 6770.
(50) Ruh, R.; Corfield, P. W. R. *J. Am. Ceram. Soc.* **1970**, *53*, 126.
(51) Hansson, M. *Acta Chem. Scand.* **1969**, *23*, 3541.
(52) Kuznetsov, V. Y.; Dikareva, L. M.; Rogachev, D. L.; Nikolaev, V. P.; Porai-Koshits, M. A. *J. Struct. Chem.* **1984**, *25*, 968.
(53) Skanthakumar, S.; Antonio, M. R.; Wilson, R. E.; Soderholm, L. *Inorg. Chem.* **2007**, *46*, 3485.
(54) Mumme, W. G. *Acta Crystallogr., Sect. B* **1971**, *27*, 1373.
(55) Rogachev, D. L.; Dikareva, L. M.; Nikolaev, V. P.; Kuznetsov, V. Y. *J. Struct. Chem.* **1981**, *22*, 473.
(56) Rogachev, D. L.; Dikareva, L. M.; Kuznetsov, V. Y.; Fomenko, V. V.; Porai-Koshits, M. A. *J. Struct. Chem.* **1982**, *23*, 765.
(57) Kuznetsov, V. Y.; Rogachev, D. L.; Dikareva, L. M.; Porai-Koshits, M. A. *J. Struct. Chem.* **1985**, *26*, 225.
(58) Kuznetsov, V. Y.; Rogachev, D. L.; Gusev, A. I.; Chuklanova, E. B. *Soviet Physics—Crystallography* **1991**, *36*, 328.
(59) Schulze, H.; Weinstock, N.; Muller, A.; Vandrish, G. *Spectrochim. Acta, Part A* **1973**, *29A*, 1705.
(60) Nakamoto, K. *Infrared and Raman Spectra of Inorganic and Coordination Compounds: Theory and Applications in Inorganic Chemistry;* Wiley: Hoboken, NJ, 1997; pp 424.
(61) Rudolph, W. W.; Fischer, D.; Tomney, M. R.; Pye, C. C. *Phys. Chem. Chem. Phys.* **2004**, *6*, 5145.
(62) Baglin, F. G.; Breger, D. *Inorg. Nucl. Chem. Lett.* **1976**, *12*, 173.
(63) Kanazhevskii, V. V.; Shmachkova, V. P.; Kotsarenko, N. S.; Kolomiichuk, V. N.; Kochubei, D. I. *J. Struct. Chem.* **2006**, *47*, 860.